Earth and Planetary Science Letters

Ancient refractory asthenosphere revealed by mantle re-melting at the Arctic Mid Atlantic Ridge

--Manuscript Draft--

Manuscript Number:	EPSL-D-20-01722
Article Type:	Letters
Keywords:	Nd-Hf isotopes; Mid Ocean Ridge Basalts; depleted mantle; Knipovich Ridge; magma mixing
Corresponding Author:	Alessio Sanfilippo Universita' degli Studi di Pavia Pavia, ITALY
First Author:	Alessio Sanfilippo
Order of Authors:	Alessio Sanfilippo
	Vincent J.M. Salters
	Sergey Y. Sokolov
	Alexander A. Peyve
	Andreas Stracke
Abstract:	The upper mantle is a heterogeneous mixture of refractory and recycled crustal domains. The recycled portions, more fertile and thus preferentially melted, dominate the composition of the basalts erupted on the surface, whereas the imprint of melting of the refractory counterparts is difficult to discern from the basalt chemistry. Contrasting radiogenic isotopic signatures of mid-ocean ridge basalts and oceanic mantle, however, show that Hf isotopes have high preservation potential during magma ascent and mixing, allowing identification of depleted mantle end-members unseen in other isotope systematics in basalts. Here, we show that basalts from Mohns and Knipovich ridges, two >500-km long oblique super-segments in the Arctic Atlantic, have uniquely radiogenic Hf isotope ratios, not mirrored by comparatively depleted Nd-Sr and Pb isotopes. These compositions can only be explained if a highly depleted asthenospheric mantle melts beneath this section of the Arctic Mid Atlantic Ridge. We argue that this depleted source consists of high proportions of ancient (> 1Ga), ultra-depleted mantle, drained of enriched components before being emplaced in the oceanic lithosphere and successively re-melted in its current location following a recent ridge-jump, allowing the identification of ultra-depleted mantle components in the arctic subridge mantle.
Suggested Reviewers:	Jonathan Snow jesnow@lsu.edu Expert in petrology of abyssal peridotites and evolution of Arctic Ridges
	Jon Lassitier lassiter1@jsg.utexas.edu Expert in isotope geochemistry of abyssal peridotites and MORB
	Eric Hellebrand e.w.g.hellebrand@uu.nl Expert in mantle geochemistry and petrology of mid ocean ridges
	Jessica Warren warrenj@udel.edu Expert in geochemistry of abyssal peridotites and MORB
	Sarah Lambart sarah.lambart@utah.edu Expert in mantle melting and geochemistry of MORB
Opposed Reviewers:	

Ancient refractory asthenosphere revealed by mantle re-melting at the Arctic Mid Atlantic Ridge

Alessio Sanfilippo*[1], Vincent J.M. Salters[2], Sergey Y. Sokolov[3], Alexander A. Peyve[3], Andreas Stracke[4]

1- Dipartimento di Scienze della Terra e dell'Ambiente, University of Pavia, Pavia, Italy
2- Department of Earth Ocean Atmospheric Science and National High Magnetic Field Laboratory, Florida State University, Tallahassee, Florida, USA
3- Geological Institute, Russian Academy of Science, Moscow, Russia
4- Institut für Mineralogie, Westfälische Wilhelms-Universität, Münster

* Corresponding author email: *alessio.sanfilippo@unipv.it*

ABSTRACT

The upper mantle is a heterogeneous mixture of refractory and recycled crustal domains. The recycled portions, more fertile and thus preferentially melted, dominate the composition of the basalts erupted on the surface, whereas the imprint of melting of the refractory counterparts is difficult to discern from the basalt chemistry. Contrasting radiogenic isotopic signatures of mid-ocean ridge basalts and oceanic mantle, however, show that Hf isotopes have high preservation potential during magma ascent and mixing, allowing identification of depleted mantle end-members unseen in other isotope systematics in basalts. Here, we show that basalts from Mohns and Knipovich ridges, two >500-km long oblique super-segments in the Arctic Atlantic, have uniquely radiogenic Hf isotope ratios, not mirrored by comparatively depleted Nd-Sr and Pb isotopes. These compositions can only be explained if a highly depleted asthenospheric mantle melts beneath this section of the Arctic Mid Atlantic Ridge. We argue that this depleted source consists of high proportions of ancient (> 1Ga), ultra-depleted mantle, drained of enriched components before being emplaced in the oceanic lithosphere and successively re-melted in its current location following a recent ridge-jump, allowing the identification of ultra-depleted mantle components in the arctic subridge mantle.

Keywords: Nd-Hf isotopes, Mid Ocean Ridge Basalts, depleted mantle, Knipovich Ridge, magma mixing

1. INTRODUCTION

The upper mantle is a complex assemblage of peridotites and recycled materials with variable age and compositions, which testify to a long-term history of partial melting and re-fertilization during Earth history. Mid Ocean Ridges Basalts (MORB) and Ocean Island Basalts (OIB) originate by partial melting of this heterogeneous mantle source and thus provide indirect evidence about mantle composition and evolution (e.g., Allegre et al., 1984; Zindler and Hart, 1986; Schilling et al., 1992; Goldstein et al., 2008; Meizen et al., 2010; Stracke, 2012). However, to what extent the compositional variability is transferred from mantle to melts erupted on the surface depends on the way partial melts samples the Earth's mantle and the style and extent of melt mixing prior to eruption. In general, mixing processes introduce a sampling bias such that the incompatible element budget of the melts is dominated by the most enriched, or least depleted, source components (i.e., Stracke and Bourdon, 2009; Stracke, 2012; Rudge et al., 2013; Lambart et al., 2012; Warren, 2016; Liu and Liang, 2017). This compositional bias is also inversely related to the overall degree of depletion (Salters et al., 2011), that is, the more refractory the mantle components are, the less they contribute to the overall incompatible element budget of the generated melts (see also Harvey et al., 2006; Liu et al., 2008; Warren and Shirey, 2012; Dai et al., 2017; Willig et al., 2019). This effect also applies to the long-lived radiogenic isotope ratios of the Rb-Sr, U-Th-Pb, Sm-Nd, and Lu-Hf decay systems. If different portions of the mantle evolve without extensive isotopic equilibration, they develop increasingly different isotope ratios (Hofmann and Hart, 1978). The isotopic compositions of these most depleted domains of the mantle sources, however, are easily concealed by mixing with melts from more enriched components (e.g., Stracke and Bourdon, 2009; Salters et al., 2011; Stracke, 2012; Rudge et al., 2013; Liu and Liang, 2017; Lambart et al., 2019). As a result, the contribution of highly depleted portions of the mantle is likely to be grossly underestimated (Harvey et al, 2006; Stracke et al., 2011; 2019; Warren and Shirey, 2012; Stracke, 2012; Byerly and Lassitier, 2014; Dai et al., 2017; Willig et al., 2019).

Another fundamental effect is that the isotopic signal of the source will be recorded differently for the different isotope systems, because the daughter elements of the most commonly used decay systems (Rb-Sr, U-Th-Pb, Sm-Nd, and Lu-Hf) are variably incompatible. For instance, mantle melting fractionates Lu/Hf more than Sm/Nd, so that the residual mantle will develop a more pronounced isotopic record of depletion for Hf compared to Nd isotope ratios (Salters and Zindler, 1995; Blichert-Toft et al., 2005; Stracke et al., 2011). In addition, Hf is significantly less incompatible than Nd during mantle melting (e.g., Hoffman, 2007), so that the difference in concentration between melts and depleted mantle is much less for Hf than for Nd. Hence, high Hf isotope ratios expected for depleted source components have higher chances to be preserved during magma ascent and mixing. Based on this rationale, and in agreement with the evidence that clinopyroxenes from abyssal peridotites locally exhibit Nd and Hf isotope ratios that are more radiogenic than those of the associated basalts (Salters and Dick, 2002; Bizimis et al., 2003; Cipriani et al., 2004; Stracke et al., 2011; Byerly and Lassitier, 2014; Mallick et al., 2014; Warren, 2016; Liu and Liang, 2017; Lambart et al., 2019), geochemical models (Salters et al., 2011; Sanfilippo et al., 2019) suggest that high and variable $^{176}Hf/^{177}Hf$ at a given $^{143}Nd/^{144}Nd$ in the most depleted MORB may result from a comparatively higher contribution of melts from ancient, ultra-depleted source components.

Here, we report new analyses of Nd-Sr-Pb-Hf isotopes of basalts collected from the northern region of Knipovich ridge (77-78 ºN), which, in combination with literature data, result in detailed coverage of the compositional variability of basalts from the Arctic ridges. These data suggest that an, on average, highly depleted mantle asthenosphere is currently located below the Knipovich and Mohns ridges. We argue that this mantle domain consists of large proportions of ancient, ultra-depleted material interspersed with small proportions of variably depleted lithologies. This parcel of North Atlantic mantle was scavenged of the most fertile lithologies when melted along the paleo-Mohns and paleo-Knipovich axes, and successively re-melted in its current location after a recent ridge-jump that occurred in the last 5 Ma.

2. MANTLE SEGMENTATION IN THE ARCTIC REGION

The Mid Ocean Ridges of the Arctic vary significantly in segment length, spreading rate, obliquity, axial depth and inferred thickness of the magmatic crust. All these parameters are primarily related to the extent and style of melt production. The spreading rate is very slow at Kolbeinsey and Mohns ridges (18–16 mm/yr) (Mosar et al., 2002; Breivik et al., 2006), and decreases to ultraslow (<13 mm/yr) at Knipovich and Gakkel Ridges (Michael et al., 2003; Goldstein et al., 2008). The spreading direction changes from nearly orthogonal in Kolbeinsey and Gakkel (Mosar et al., 2002), to highly oblique (up to ~50°) at the Mohns and Knipovich (Okino et al., 2002) ridges (Fig.1). As a consequence, the Knipovich Ridge consists of a series of small pull-apart basins with sparse magmatic activity on the seafloor (Okino et al., 2002; Yampolski and Sokolov, 2003; Sokolov et al., 2011). The crustal thickness decreases progressively northward, from a 7-8 km-thick magmatic crust at the Kolbeinsey Ridge, to almost zero at Gakkel Ridge where large sections of mantle are directly exposed on the ocean floor (Dick et al., 2003).

The geochemistry of the basalts from the Arctic ridges has been extensively studied and is depicted in figure 2 (Schilling et al., 1983; 1999; Neumann and Schilling, 1984; Waggoner et al., 1989; Mertz et al., 1991; 2004; Devey et al., 1994; Haase et al., 1996; 1997; Mertz et al., 1997; Trønnes et al., 1999; Michael et al., 2003; Blichert-Toft et al., 2005; Goldstein et al., 2008; Elkins et al., 2011; 2014; Nauret et al., 2011). The gradual decrease in spreading rates from Kolbeinsey to Mohns and Knipovich Ridge is mirrored by an overall increase in Na_8 (that is, Na_2O normalized to 8 wt% MgO) (Klein and Langmuir, 1987) and by changes in trace element ratios that mostly depend on melting conditions. For instance, there is an obvious increase in the ratio between the middle and heavy rare earth elements (M/HREE, e.g., Gd/Yb) from Kolbeinsey towards Knipovich Ridge, which suggests a larger proportion of melt generated in the garnet stability field. The high $^{230}Th/^{238}U$ ratios in these basalts (Elkins et al., 2014) may also be due to the effect of thickening the lithospheric lid, as a result of decreasing spreading rates. At closer inspection, however, the basalt compositions identify different domains, which indicate a strong segmentation of the mantle in this region. The most obvious variations are defined by the radiogenic isotope ratios, through which we will hereafter describe the depleted or enriched nature of the mantle source (where "depletion" refers to time-integrated incompatible element depletion reflected in low $^{87}Sr/^{86}Sr$ and $^{206, 207, 208}Pb/^{204}Pb$, but high $^{143}Nd/^{144}Nd$ and $^{176}Hf/^{177}Hf$; the converse applies to "enriched" isotope signatures).

Figure 2 shows that a geochemically enriched mantle source is likely located beneath the Jan Mayen Fracture Zone, and dispersed into the neighboring ridges (Haase et al., 1996). These lavas are characterized by strong enrichments in incompatible elements (e.g., high La/Sm) and have the lowest Hf and Nd isotope compositions of all Arctic ridge basalts, thus suggesting the occurrence of a mantle section that is isotopically distinct from Iceland (Blichert-Toft, 2005). The dispersion of this geochemically enriched material is seen in the basalts from the northern part of Kolbeinsey Ridge as well as those from western Mohns Ridge (e.g, Schilling et al., 1983; 1999; Neumann et a., 1984; Waggoner et al., 1989; Haase et al., 1996) although detailed analyses of Pb isotope ratios reveal a sharp geochemical boundary south of the Mohns FZ (Blichert-Toft et al., 2005). Excluding the geochemically enriched compositions related to the influence of the Jan Mayen FZ "plume", basalts from Kolbeinsey Ridge are characterized by incompatible element depletions and radiogenic Nd and Hf isotope ratios. Along with a low Na8 and low Gd/Yb ratios these data are indicative of high degrees of melting of a shallow, depleted asthenosphere, which consists of depleted peridotite plus minor heterogeneities mainly derived from recycled oceanic material (e.g., Mosar et al., 2002; Elkins et al., 2014).

Another obvious geochemical discontinuity is located along the Lena Trough, which represents an oceanic-continent transitional rift zone where volcanism is mainly localized in a southern and a northern region (Snow et al., 2007). At Lena south, K-rich alkali basalts show peculiar enrichments in highly incompatible trace elements, strong HREE fractionation and high Sr and low Nd isotope ratios, whereas Pb isotopes and Na8 are characteristically low (Fig. 3) (Nauret et al., 2011). These features have been related to the occurrence of subcontinental lithosphere, possibly phlogopite/amphibole- and garnet-bearing, in the source of these basalts (Laukert et al., 2014). The enrichments in Sr and Nd isotope ratios are attenuated towards the northern part of Lena Trough, where the geochemical fingerprint of the volcanism is similar to that of the basalts from the western volcanic zone of Gakkel Ridge (WVZ). Both series are characterized by relatively enriched Sr and Nd isotope ratios and by a strong a DUPAL-like Pb isotope anomaly of high $^{207}Pb/^{204}Pb$ (Goldstein et al., 2008). These features have been related to the occurrence of subcontinental lithospheric mantle (SCLM) in their source, most likely delaminated during the opening of the slow-spreading oceanic basin (Goldstein et al., 2008). On the other hand, the basalts in east Gakkel Ridge (East Volcanic Zone, EVZ) are depleted in trace elements and in all isotope ratios, which suggest moderate to low degrees of melting of a depleted mantle source, similar to the typical North Atlantic mantle (Goldstein et al., 2008; Elkins et al., 2014). In this framework, the basalts from Mohns and Knipovich Ridge define geochemical trends distinct from Kolbeinsey and Gakkel Ridge basalts (Figs 2, 3)

(Blichert-Toft et al., 2005, Elkins et al., 2014) and are thought to be sourced by a similar depleted mantle asthenosphere, bordered by two geochemical discontinuities located along the Jan Mayen FZ and Lena Trough.

3. MATERIALS AND METHODS

New isotopic data were obtained for basalt glasses and whole-rocks collected from the northernmost parts of Knipovich Ridge (77º-78ºN), which connects to Lena Trough through the Molloy FZ. Samples were collected during cruise 24 of the Akademik Nikolaj Strakhov (2006), and dredged either from the rift valley or rift flanks. A thorough textural description and major and trace element compositions of these samples are reported in (Sushchevskaya et al., 2010), and summarized in Table S1. The basalts are aphyric to weakly olivine-phyric and have high-MgO (8.6-14.8 wt%) and low incompatible element contents, indicating that these basalts are near-primitive melts. Their primitive nature is also confirmed by the high olivine Fo contents (>88.5 mol%) of phenocrysts and by the nearly complete absence of plagioclase. Basalts are locally subalkalic ($Na_2O + K_2O = 2.8\text{-}4.1$ wt%), and have large variations in Na8 (2.0-4.0). Incompatible trace element compositions vary from depleted to slightly enriched (La/Sm=0.8-2.7) and are characterized by variable M/HREE fractionations (Gd/Yb=1.3-2.1) (Fig. 2).

New Nd-Hf-Sr-Pb isotopic determinations were performed at the National High Magnetic Field Laboratory, Florida State University following the method described in detail in (Mallik et al., 2014), and are reported in Table S1 of the supplementary material. We digested approximately 100 mg of powder, which was leached at room temperature with 2.5 N HCl for about 15-20 min. The leached fraction was rinsed several times using 18MΩ deionized water and then QD (quartz distilled) water and finally dissolved in a HF: HNO3 (3:1) mixture. Lead, Hf, Sr and Nd were separated from the same aliquot following the techniques outlined in Mallik et al. (2014). Sr isotope ratios were measured by thermal ionization mass spectrometer (TIMS) in dynamic mode on a Finnigan MAT 262 RPQ mass spectrometer.

$^{87}Sr/^{86}Sr$ ratios are corrected for fractionation to $^{86}Sr/^{88}Sr$ = 0.1194. Long-term average of Sr standard E & A yields a value of 0.708004 ± 12ppm (n=25, 2 S.D.). $^{86}Sr/^{88}Sr$ of the samples are reported relative to the accepted ratio of E & A standard ($^{87}Sr/^{86}Sr$ = 0.70800). Nd-Pb-Hf isotope ratios were measured on a ThermoFinnigan NEPTUNE MC-ICP-MS. $^{143}Nd/^{144}Nd$ ratios are corrected for fractionation to $^{146}Nd/^{144}Nd$ = 0.7219. $^{176}Hf/^{177}Hf$ ratios are corrected for fractionation to $^{179}Hf/^{177}Hf$ = 0.7325. Ratios are reported relative to $^{176}Hf/^{177}Hf$ =0.282160 for standard JMC-475. Reproducibility of the basalt data is generally better than 10ppm. $^{143}Nd/^{144}Nd$ are reported relative to 0.511858 for the the LaJolla standard (Lugmair and Carlson, 1978). Pb isotope ratios were measured using a Tl spike to correct for mass fractionation with ratios corrected to $^{203}Tl/^{205}Tl$ = 0.4188. Samples and standard were spiked with Tl to obtain a Pb/Tl ratio of approximately 6. Reproducibility of the Pb-isotope ratios is better than 123ppm for $^{206}Pb/^{204}Pb$; 164 ppm for $^{207}Pb/^{204}Pb$ and 211 ppm for , $^{208}Pb/^{204}Pb$. Pb isotope ratios are reported relative to the accepted values of NBS 981 ($^{206}Pb/^{204}Pb$ =16.9356, $^{207}Pb/^{204}Pb$= 15.4891, $^{208}Pb/^{204}Pb$= 36.7006).

5. RESULTS

The samples show highly radiogenic and rather uniform $^{176}Hf/^{177}Hf$ isotope ratios (0.28211-0.28343) associated to variable $^{143}Nd/^{144}Nd$ (0.51311-0.51343), $^{86}Sr/^{87}Sr$ (0.7027-0.7031) and $^{206}Pb/^{204}Pb$ (17.81-18.86) isotope ratios (Fig. 2). The Hf, Nd, Sr and Pb isotopic compositions are overall well interrelated, and correlate with the LREE/MREE and MREE/HREE ratios (see Fig. 4 and Fig.S2 in supplementary files). Overall, our new data are consistent with published data from the southern portion of Knipovich Ridge and the eastern part of Mohns Ridge (defined 'E-Mohns' in figures 1 to 5). They have relatively high incompatible trace element ratios (i.e., La/Sm) and variable Sr and Pb isotopes, which are coupled with strongly radiogenic Nd and Hf isotopes. In particular, Nd, Sr and Pb isotope compositions of the Knipovich and E-Mohns basalts range between "DM-like" values (Salters and Stracke, 2004) and mildly enriched compositions similar to those of the Jan Mayen FZ (Figs. 2, 3). Nonetheless, basalts from both ridges have extremely high $^{176}Hf/^{177}Hf$ ratios that exceed those of MORB in the region, suggesting the existence of a depleted end-member having strongly radiogenic Hf isotopes (see also Blicher-Toft et al., 2005). Our new data thereby confirm that this prominent shift in Hf isotopic ratios characterizes an entire ~1000 km-long sector of Arctic MAR, ranging from the Jan Mayen FZ until the connection between Knipovich Ridge and Lena Trough. Hence in figure 4, the basalts from Knipovich and E-Mohns ridges form correlation lines parallel to those of the other ridges nearby, but at constantly higher Hf isotopic ratios.

6. DISCUSSION

6.1 A highly depleted mantle domain at Knipovich and Mohns Ridges

The basalts from Lena and WVZ in Gakkel are thought to reflect a high proportion of subcontinental mantle in their source, and are the only basalts from the North Atlantic with a DUPAL-type signature (Goldstein et al., 2008; Elkins et al., 2011; 2014). Hence, it has been can argued that the overall high $^{176}Hf/^{177}Hf$ in E-Mohns and Knipovich basalts may also derive from melting stripes of delaminated subcontinental mantle with old depletion signatures (Blichert-Toft et al., 2005). Although the most enriched basalts of Knipovich and E-Mohns have similar Nd and Sr isotope ratio and trace element compositions to the most depleted basalts from Lena north and WGV, they do not have such high Hf isotope ratios.

Hence, the basalts at Knipovich and E-Mohns Ridge sample a distinct depleted mantle component. Moreover, the SCLM sourcing Lena and WGV basalts is characterized by high Rb/La and radiogenic Sr isotopes, but very low $^{206}Pb/^{204}Pb$ (Fig. 3). These compositions require the occurrence of mica or amphibole in their source, and further support the idea of a metasomatized subcontinental lithosphere akin that beneath the Svalbard as source of basalts in Lena Trough and WGV (Snow et al., 2007; Nauret et al., 2011; Laukert et al., 2014). Low Pb isotope ratio and high Rb/La are not observed in the basalts from Knipovich and Mohns Ridge (see also Goldstein et al., 2008), which instead tend towards the isotopic compositions of the basalts from the Jan Mayen FZ (Fig. 3). Moreover, we must note that if there is a gradual chemical transition from Mohns to the enriched mantle source of Jan Mayen, our new data show that the transition from the source of Knipovich and the enriched mantle of Lena Trough is abrupt, which further questions the possible contribution of SCLM south of 79ºN of latitude (Fig. 2). The ~600 km-long Lena Trough, which separates the Knipovich and Gakkel Ridge, is therefore not simply a tectonic reflection of an ultraslow spreading seafloor (Dick et al., 2003), but represents a sharp compositional boundary between a northern mantle domain characterized by the presence of delaminated portions of SCLM and a southern domain, on average strongly depleted in Hf isotopes and influenced towards the south by the dispersion of enriched material located beneath the Jan Mayen FZ.

Stracke et al. (2019) recently found evidence for ultra-depleted melts with higher Nd isotope ratios than observed for oceanic basalts so far, in olivine-hosted melt inclusions in basalts from the Azores. These Nd isotope ratios are comparable to the most radiogenic $^{143}Nd/^{144}Nd$ observed in abyssal peridotites, and similar to those of highly refractory peridotites locally found at MOR (Harvey et al., 2006; Liu et al., 2008; Stracke et al., 2011; Byerly and Lassitier, 2014; Day et al., 2017; Urann et al., 2020). More importantly, the preservation of such extremely radiogenic isotope ratios in melt inclusions (nonetheless partly mixed with more enriched melts) requires that this ancient and ultra-depleted material in the asthenosphere must be abundant, because mixing and aggregation of such ultra-depleted melts with more enriched melts easily erases the depleted isotope signatures (see also Stracke and Bourdon, 2009). Sanfilippo et al. (2019), came to similar conclusions and, following earlier models (Salters et al., 2011; Byerly and Lassitier, 2014), argued that Hf isotopic ratios in basalts may even better preserve extreme isotopic signature of a depleted mantle compared to the more incompatible Nd, Sr and Pb, although also partly dampened by mixing with enriched lithologies. From this perspective, the consistently higher Hf isotope ratios in basalts from Knipovich and E-Mohns Ridge compared to basalts from Kolbeinsey Ridge, Lena Trough and Gakkel Ridge (Fig. 2,4) may indicate a high contribution of ultra-depleted melts from ancient refractory mantle components, which will be evaluated quantitatively in the following.

6.2 Contribution of melts from ancient, depleted mantle: a geochemical model

The upper mantle is probably a complex mixture of variably depleted, residual peridotites and enriched lithologies, i.e., re-fertilized peridotites or pyroxenites (see for instance Liu et al., 2008; Stracke et al., 2011; Sanfilippo et al., 2019; Lambart et al., 2019). The simplest way to simulate melting of such a heterogeneous mantle source is by melting a three-component mantle formed by: (1) an ancient, refractory peridotite end-member, which produces an ultra-depleted melt (UD_Melt); (2) a less depleted peridotite with a “DM-like” composition that forms a MORB-like melt (D_melt) (3) a geochemically enriched source, possibly representing pyroxene-rich, recycled component and producing a melt with geochemically enriched trace element and isotopic compositions (E_melt). Melts from these three mantle end-members are variably mixed to reproduce the correlations observed in the Arctic ridge basalts (further details of the model are given in the supplementary files). For simplicity, the composition of E_melt is the average of the geochemically enriched basalts from the Jan Mayen FZ, which are considered to sample a single mantle component (Haase et al., 1996; Blicher-Toft et al., 2005) ubiquitously found in ocean floor basalts (Hanan et al., 2000; Stracke et al., 2005). The D_melt and UD_melt are produced with a dynamic melting model described in detail in the supplementary material. This melting model follows the same rationale of Salters et al. (2011); Sanfilippo et al. (2019) and Willig et al., (2020), who intended to reproduce correlation lines of MORB in the Nd-Hf-Ce isotopic space; and is now expanded here to include the Sr and Pb isotope ratios and trace elements. The D_melt is produced by 10% melting of a depleted peridotite having DM compositions from Salters and Stracke (2004). The UD_melt is produced by melting a source having ultra-depleted, refractory compositions, which are in turn acquired during ancient melting events (spanning from 0.5 to 2 Ga in our model) of a DM source. In detail, the trace element and isotopic compositions of this refractory source were calculated as weighted sum of single melting intervals (each interval corresponding to F=0.2) of a triangular melting region residual from a DM-type mantle melted for F=15% (see supplements). Melts and source compositions are shown in Fig. 5, which illustrates the diversity of the three end-members in terms of trace element and Nd-Hf-Sr-Pb isotope compositions (see also Table SM2).

Given the depleted character of the UD_Melt (see Table SM2), its isotopic signatures are easily concealed even at low extents of mixing, resulting in convex mixing lines in the Hf vs Nd, Sr and Pb spaces (Fig. 5b). At the scale of figure 4, however, these mixing lines appear almost vertical. Consequently, the different correlation lines of basalts from the Arctic ridges in the Hf vs Nd-Sr-Pb-La/Yb space can be explained with an overall higher contribution of melts from an ancient, refractory source, having an extreme isotopic signal. To account for these parallel trends, our model suggests that the contribution of this depleted material must be nearly constant at the scale of each ridge segment. This implies that the basalts sample the contribution of melts form the ancient mantle remains constant, but the enriched and less depleted lithologies are sampled in variable proportions (see also Sanfilippo et al., 2019; Willing et al., 2020). For a depletion age of 1 Ga, consistent with the average Re depletion ages of the ancient, refractory peridotites sampled at Gakkel Ridge (Liu et al., 2008; Stracke et al., 2011; Day et al., 2017) our mixing model requires a contribution of ultra-depleted melts in the MORB mixture of Mohns and Knipovich basalts ranging between 20 and 30%, twice higher than those in the neighboring Kolbensey ridge (Fig. 4). Any change in the isotopic compositions of the E-melts and D-melts has a minor effect on the results of our model, which would produce lines parallel to the trends defined by each section (see for instance Fig. 4a). On the other hand, the use of different ages of mantle depletion would modify the isotope ratios of the UDM. This modifies the proportions of the ultra-depleted melts in the MORB mixture for the basalts of E-Mohns and Knipovich to a minimum estimate of 10% and a maximum estimate of 40%, for 2Ga and 0.5Ga depletion ages respectively (Fig. 4a). Independent of the age of depletion of the ultra-depleted source, the contribution of ultra-depleted melts in the MORB mixture of Mohns and Knipovich basalts remains two times higher than that in the more typical MORBs of Kolbeinsey Ridge (see Fig. 4). Changes in the absolute concentration of each element (i.e., Hf, Nd, Sr, Pb, La, Yb) in the three melts would also modify their proportions in the MORB mixture, but this would not modify the convex shape of the mixing lines in the Hf vs Nd-Sr-Pb-La/Yb spaces. Hence, although we recognize that the choice of melting parameters (e.g., critical porosity, amount of melt generated per the depth interval, partition coefficients), source compositions and age of depletion may strongly affect the overall estimates of the contribution of the three end-members in the MORB mixture, our model indicates that the parallel correlation lines seen in the Hf vs Nd, Sr, Pb and La/Yb spaces requires different proportions of UD-Melt in the MORB mixture of the different ridge segments. On this basis, we infer that the prominent shift in Hf isotopic ratios towards radiogenic compositions in Mohns and Knipovich Ridge is a consequence of an overall higher amount of ancient, refractory material in this parcel of the North Atlantic asthenosphere.

6.3 Ridge jump and mantle re-melting

The formation of the Arctic oceanic basins started at ~55 Ma, by rifting between Greenland and Eurasia that initially formed the Aegir, Jan Mayen, Mohns, and Gakkel Ridges. The Jan Mayen FZ connected Mohns with an early Kolbeinsey Ridge, following a ridge jump and the final deactivation of Aegir Ridge (Bott, 1985). The formation of early Knipovich Ridge occurred in the early Oligocene as consequence of a change in spreading direction of the Mohns and Gakkel Ridges from NNW-SSE to NW-SE (Gusev and Shkarubo, 2001). However, the high obliquity of the present-day Knipovich axis (41º to 55º from the spreading direction) and its vicinity to the Norwegian continental shield (see Fig. 1) led previous authors to suggest that the present-day Knipovich Ridge is an intra-oceanic rift resulting from rift jumps or breakup under conditions of shearing (Vogt, 1978; Sokolov, 2011; 2014). The anomalous structure of this super-segment is obvious from its geometry, which is unlike a typical spreading center, and more similar to a series of pull-apart basins which are divided by highs perpendicularly to the spreading direction (Okino et al., 2002; Sokolov et al., 2011).

Oceanic rifting is mostly supported by the geometry of the linear anomalies in the magnetic field, which although partly obscured by the thick sedimentary cover, are oriented at high angle (~45º) to the present ridge direction (Olesen et al., 1997) suggesting a recent change in spreading direction (see Fig. S2 in supplement). Geodynamic reconstructions of the opening of the Greenland – Norway rift, which indicate an abrupt change of the plate separation direction in the late Pliocene (< 5 Ma) (Mosar et al., 2002; Sokolov, 2011; 2014), further support a recent ridge jump, in addition to the anomalously thick and consolidated sedimentary cover (Vogt et al., 1978; Crane et al., 2001) which overlays the present-day axis. During recent cruises by Russian vessels (cruise 19 of the R/V Professor Logachev and cruise 24 of the R/V Akademik Nikolaj Strakhov), geophysical surveys indicated that the thick and consolidated sediments exposed along the axis are crosscut by active faults with angles up to 35º (Sokolov, 2011; Yampolskiy and Sokolov, 2012; Sokolov et al., 2014). Dredging in these locations revealed the occurrence of partly consolidated argillites locally cut by fresh basalts and dated on the basis of paleontological association to the late Oligocene (Bugrova et al., 2010). Similarly, DSDP Hole 344 (located ~25 km in the east flank of the ridge at ~76ºN) recovered gabbros and diorites with ages >3 Ma younger than the overlying sediments, probably of upper Miocene to early Pliocene age. Although unambiguous evidence for an abandoned rift axis west of Knipovich are still lacking, all these data indicate a re-adjustment of the Knipovich axis towards the east in the late Pliocene.

The prominent shift in Hf isotope ratios observed at Knipovich Ridge also extends to basalts from east Mohns Ridge. Here, the magnetic anomalies are coherent with the direction of the Mohns axis, and a well-developed positive anomaly delimits the present-day ridge. The magnetic anomalies at Mohns Ride are, however, very poorly defined for the interval from ~60 km on the southern flank to ~75 km on the northern flank from the present axis, and the continuity of Mohns with the present-day Knipovich Ridge indicates that the two ridges align since relocation of the latter to its present position. The distance between Mohns axis and the 5C magnetic anomaly is 25% greater in the northwest flank compared to the southeast flank (Vogt et al., 1978). It is thereby plausible that the change in spreading direction of Knipovich Ridge coincided with a synchronous translation of the Mohns spreading axis. A jump of the Mohns spreading axis towards the south-east, which is parallel to the existing ridge axis, would not have produced any change in the orientation of the recent magnetic anomalies. In addition, since this ridge jump must have likely occurred within the last 5 Ma - and assuming a spreading rate of 15 mm/yr - Mohns should have produced no more than ~ 35 km of new oceanic lithosphere in the present location, accounting for the well-developed, recent magnetic fabric. The possibility that the Mohns ridge axis might have jumped towards the southeast is in agreement with the observation of Vogt (1978) that the highest rift mountain topography and shallowest basement occurring on the west of the Mohns ridge axis, although subsidence is expected to be a regular function of time and distance to the ridge axis (e.g., Sclater et al., 1971).

A recent ridge jump of the Knipovich and Mohns axes may also explain the anomalous depleted character of this portion of the Arctic mantle. Melting a heterogeneous mantle decreases preferentially the amount of enriched lithologies, in turn resulting in an overall higher proportion of the most depleted end members. As a result, material that is emplaced at shallower depths and transported laterally with the newly formed lithosphere will have an overall higher proportion of refractory mantle, whereas the proportion of the enriched/ or less depleted components is lower due to preferential melting during the earlier melting episode (Fig. 6). Successive adjustments in ridge axis, such as the opening of intra-transform domains (Graham and Michael, 2020; Sani et al., 2020) or a jump in ridge axis, may cause this depleted portion of oceanic upper mantle to melt a second time, until new asthenosphere is gradually emplaced in the melting column. Owing to the ultra-slow spreading rates (<13 mm/yr) and the recent ages of the Knipovich ridge adjustment (< 5 Ma), this depleted mantle source will be re-processed before new, fresh asthenosphere is emplaced in the melting region (Fig. 6), leading to production of isotopically highly depleted basalts. Specifically, for a mantle upwelling that equals the present-day (half)spreading rates, more than 14 Ma would be required to entirely replace the depleted material with more ‘tyical’ asthenosphere in the melting region of Knipovich and Mohns Ridges (considering a depth of ~100 km). We note that the basalts from Knipovich and Mohns Ridges display a northward increase in Na8, LREE/MREE and MREE/HREE fractionations, associated to scattered and locally high Sr and Pb isotopic signals (Blicher-Tpft et al., 2002) (Fig. 2) and $^{230}Th/^{238}U$ ratios (Elkins et al., 2014). Spreading rates in Mohns and Knipovich decrease northward, associated with an increase in obliquity and, therefore, in a gradual decrease in the overall degrees of partial melting, coupled with a deepening of the minimum melting pressure. The main consequence of these variations is the preferential melting of fertile, chemically enriched lithologies deep in the melting column and the local production of MORBs having relatively high La/Sm ratios and locally radiogenic Sr and Pb isotopic signatures (see Fig. 4).

The last remaining issue is whether ancient, refractory domains of the mantle can melt after being emplaced at lithospheric levels within the mantle column. In particular, given that most of the incompatible element budget of a mantle peridotite is retained in clinopyroxene (Stracke et al., 2011), the ability of such refractory portions to transfer their isotopic signals to the primary melts is certainly limited. Using *pMELTS* calculations, Byerly and Lassitier (2014) have shown that an ancient, refractory lithosphere with compositions akin to the refractory peridotites from Gakkel Ridge (Liu et al., 2008; Stracke et al., 2011; Day et al., 2017) and Salt Lake Crater (Hawai’i) (Bizimis et al., 2003) can produce up to 10% and 5% of melts, respectively, before exhaustion of clinopyroxene, for typical mantle potential temperatures of 1350ºC. Sani et al. (2020) recently implemented this calculation considering mantle potential temperatures of 1325 °C, 1350 °C and 1375

°C. In detail, these authors used a starting pressure of 15 kbar and a final pressure of 5 kbar, for a mantle adiabat of ~0.8ºC/km, showing that sources with refractory compositions (i.e., residual after 5% to 10% melting of a DM-mantle) can produce significant amounts of melts (up to 12% and 7%, respectively) before exhaustion of clinopyroxene; independent of the mantle potential temperature (see Fig.11 in Sani et al., 2020). Since mantle melting fractionates Lu/Hf more than the other parent-daughter ratios of the common decay systems (i.e., Sm/Nd, Rb/Sr, U-Th/Pb) - an effect further amplified if melting in the presence of garnet - a clinopyroxene-bearing residual mantle will develop a more pronounced isotopic record of depletion for $^{176}Hf/^{177}Hf$ compared to the other isotopic ratios (Blichert-Toft et al., 2005; Salters et al., 2011; Stracke et al., 2011; Sanfilippo et al., 2019). Indeed, melting degrees between 5% and 15% will form a clinopyroxene-bearing residual peridotite with a strong radiogenic Hf fingerprint at ages of depletion of 1 Ga (see Table SM2 in supplements). This clinopyroxene-bearing, refractory mantle can therefore transfer its highly depleted isotopic fingerprint to the generated melts during a subridge melting. These inferences are entirely consistent with our melting model, which uses the triangular average trace element and isotopic compositions of a refractory mantle residual from 15% as source of the UD_Melts. A process of re-melting due to a jump in the ridge axis is thereby a viable a mechanism to melt a parcel of oceanic mantle containing high amounts of ancient ultra-depleted material. This process may thereby cause the prominent increase in Hf isotopes within the basalts produced in the newly formed ridge, although this 'depleted' isotopic signature would be unseen in Nd, Sr and Pb isotopes as well as in most incompatible trace elements.

In conclusion, the parallel correlation lines in the Hf vs Nd-Sr-Pb-La/Yb isotopic space shown by MORB form the Arctic MAR require that an ancient (>1 Ga) depleted mantle is a widespread component in the asthenosphere, but, given its highly refractory nature, its isotopic fingerprint is often concealed in derivative melts by mixing with melts from more enriched source components. The example of the Mohns and Knipovich Ridges demonstrate that tectonic processes can influence the relative amount of variably depleted lithologies in the upper mantle, allowing the identification of mantle components that have so far escaped detection.

Acknowledgments

We thank M. Ligi, E. Bonatti and R. Tribuzio for extensive discussion on a preliminary version of the manuscript. This work was financially supported by by Accordo Bilaterale CNR/RFBR 2018-2020 (CUPB36C17000250005) and by the Italian "Programma di Rilevante Interesse Nazionale" (PRIN_2017KY5ZX8) to A.S. A portion of this work was performed at the National High Magnetic Field Laboratory, which is supported by National Science Foundation Cooperative Agreement No. DMR-1644779 and the State of Florida. The geodynamic model was developed by support of RFBR 18-05-70040.

Author contributions: A.S, V.S and A.S. conceived the idea, performed the geochemical models and wrote the text; S.S. developed the geodynamic model; A.P. performed the preliminary petrological and geochemical study of the basalts; V.S. performed the isotopic determinations at FSU.

Competing interests: The authors declare that they have no competing interests.

Data and materials availability: The geochemical data on basalts from northern Knipovich used in this manuscript are provided in Table S1 as Supplementary Material. The other geochemical data are compiled from PetDb, the original references are provided in the text.

References

Allègre, C.J., Hamelin, B., Dupré, B. Statistical analysis of isotopic ratios in MORB: the mantle blob cluster model and the convective regime of the mantle. Earth Planetary Science Letters 71, 71–84 (1984).

Bizimis, M., Sen, G., Salters, V.J.M. Hf–Nd isotope decoupling in the oceanic lithosphere. constraints from spinel peridotites from Oahu, Hawaii. Earth Planetary Science Letter 217, 43–58 (2003).

Blichert-Toft, J., Agranier, A., Andres, M. , Kingsley, R., Schilling, J. G., Albarède, F. Geochemical segmentation of the Mid-Atlantic Ridge north of Iceland and ridge–

hot spot interaction in the North Atlantic, Geochem. Geophys. Geosyst., 6, Q01E19, doi:10.1029/2004GC000788 (2005).

Bott, M.H.P. Plate tectonic evolution of the Icelandic transverse ridge and adjacent regions. Journal Geophysical Research 90, 9953–9960 (1985).

Breivik, A.J., Mjelde, R., Faleide, J.I., Murai, Y. Rates of continental breakup magmatism and seafloor spreading in the Norway Basin-Iceland plume interaction. Journal Geophysical Research - Solid Earth 111, 2005JB004004 (2006).

Bugrova E. M., E. A. Gusev, and Tverskaya L. A. Oligocene rocks in the Knipovich Ridge," in Abstracts of the 14th International School of Marine Geology: Geology of Seas and Oceans (GEOS, Moscow, 2001), 1, 28–29 (2010).

Byerly, B. L., Lassiter, J. C. Isotopically ultradepleted domains in the convecting upper mantle: Implications for MORB petrogenesis. Geology, 42, 203–206 (2014).

Cipriani, A., Brueckner, H.K., Bonatti, E., Brunelli, D. Oceanic crust generated by elusive parents: Sr and Nd isotopes in basalt–peridotite pairs from the Mid-Atlantic ridge. Geology 32, 657–660 (2004).

Crane K., Doss S., Vogt P., Sundvor E., Cherkashov I.P., Devorah J. The role of the Spitsbergen shear zone in determining morphology, sedimentation and evolution of the Knipovich Ridge. Marine Geophysical Researches, 22, 153–205 (2001).

Day, JMD, Walker, R.J., Warren, J.M. 186Os-187Os and highly siderofile element abundance systematics of the mantle revealed by abyssal peridotites and Os-rich alloys. Geochimica et Cosmochimica Acta, 200, pp.232-254 (2017)

Devey C. W., Garbeschonberg C. D., Stoffers P., Chauvel C., Mertz D. F. Geochemical effects of dynamic melting beneath ridges - reconciling major and trace-element variations in Kolbeinsey (and Global) Midocean Ridge Basalt. Journal of Geophysical Research-Sol. Earth 99, 9077–9095 (1994).

Dick H. J. B., Lin J., Schouten H. An ultraslowspreading class of ocean ridge. Nature 426, 405–412 (2003).

Elkins L. J., Sims K. W. W., Prytulak J., Mattielli N., Elliott T., Blichert-Toft J., Blusztajn J., Dunbar N., Devey C. W., Mertz D. F., Schilling J. G. Understanding melt generation beneath the slow spreading Kolbeinsey Ridge from ^{238}U, ^{230}Th, and ^{231}Pa excesses. Geochimica Cosmochimica Acta 75, 6300–6329 (2011).

Elkins L.J., Sims K. W. W., Prytulak, Blichert-Toft J., Elliott T., Blusztajn J., Fretzdorff S., Reagan M., Haase K., Humphris S., Schilling J.G. Melt generation beneath Arctic Ridges: Implications from U decay series disequilibria in the Mohns, Knipovich, and Gakkel Ridges. Geochimica et Cosmochimica Acta 127, 140–170 (2014).

Goldstein S. L., Soffer G., Langmuir C.H., Lehnert K.A., Graham D.W., Michael P. J. Origin of a Southern Hemisphere geochemical signature in the Arctic upper mantle. Nature 453, 89–93 (2008).

Graham, D. W., Michael, P. J. Predominantly recycled carbon in Earth's upper mantle revealed by He-CO2-Ba systematics in ultradepleted ocean ridge basalts. Earth and Planetary Science Letters, 116646. (2020)

Gusev E.A., Shkarubo S.I. Anomalous structure of the Knipovich ridge. Russian Journal of Earth Sciences 2, 165-182 (2001).

Haase K. M., Devey C. W., Mertz D. F., Stoffers P., GarbeSchonberg D. Geochemistry of lavas from Mohns ridge, Norwegian-Greenland Sea: implications for melting conditions and magma sources near Jan Mayen. Contribution to Mineralogy and Petrology 123, 223–237 (1996).

Haase K. M., Goldschmidt B., Garbe-Schonberg C. D. Petrogenesis of tertiary continental intra-plate lavas from the Westerwald region, Germany. J. Petrol. 45, 883–905 (2004).

Harvey, J., Gannoun, A., Burton, K. W., Rogers, N. W., Alard, O., & Parkinson, I. J. (2006). Ancient melt extraction from the oceanic upper mantle revealed by Re–Os isotopes in abyssal peridotites from the Mid-Atlantic ridge. Earth and Planetary Science Letters, 244(3-4), 606-621

Hofmann, A.W. and Hart, S.R. An assessment of local and regional isotopic equilibrium in the mantle. Earth and Planetary Science Letters 38, 44-62 (1978).

Klein, E. M., Langmuir, C. H. Global correlations of ocean ridge basalt chemistry with axial depth and crustal thickness. J. Geophys. Res. 92, 8089–8115 (1987).

Lambart, S., Laporte, D., & Schiano, P. (2013). Markers of the pyroxenite contribution in the major-element compositions of oceanic basalts: Review of the experimental constraints. Lithos, 160, 14-36

Lambart S., Koorneef J.M., Millet M.A., Davies G.R., Cook M., Lissenberg J.C. Highly heterogeneous depleted mantle recorded in the lower oceanic crust. Nature Geoscience 12, 482–486 (2019).

Laukert, G., von der Handt, A., Hellebrand, E., Snow, J.E., Hoppe, P., Klügel, A. High-pressure reactive melt stagnation recorded in abyssal pyroxenites from the ultraslow-spreading Lena Trough, Arctic Ocean. Journal of Petrology 55, 427–458 (2014).

Liu, C.Z., Snow, J.E., Hellebrand, E., Brügmann, G., Von Der Handt, A., Büchl, A., Hofmann, A.W. Ancient, highly depleted heterogeneous mantle beneath Gakkel ridge, Arctic ocean. Nature 452, 311–316 (2008).

Liu, B., Liang, Y. The prevalence of kilometer-scale heterogeneity in the source region of MORB upper mantle. Science Advance, 3, e1701872 (2017).

Mallick S., Dick H.J.B., Sachi-Kocher A., Salters V.J.M. Isotope and trace element insights into heterogeneity of sub-ridge mantle Geochemistry, Geophysics, Geosystems, DOI: 10.1002/2014GC005314 (2014).

Mertz D. F., Devey C. W., Todt W., Stoffers P., Hofmann A.W. Sr–Nd–Pb Isotope evidence against plume asthenosphere mixing north of Iceland. Earth Planet. Sci. Lett. 107, 243–255 (1991).

Mertz D. F., Haase K. M. The radiogenic isotope composition of the high-latitude North Atlantic mantle. Geology 25, 411–414 (1997).

Mertz D. F., Sharp W. D. and Haase K. M. Volcanism on the Eggvin Bank (Central Norwegian Greenland Sea, latitude similar to 71 degrees N): age, source, and relationship to the Iceland and putative Jan Mayen plumes. Journal of Geodynamic 38, 57–83 (2004).

Michael P. J., Langmuir C. H., Dick H. J. B., Snow J. E., Goldstein S. L., Graham D. W., Lehnert K., Kurras G., Jokat W., Muhe R., Edmonds H. N. Magmatic and amagmatic seafloor generation at the ultraslow-spreading Gakkel ridge, Arctic Ocean. Nature 423, 956–961 (2003).

Mosar, J., Eide, E.A., Osmundsen, P.T., Sommaruga, A., Torsvik, T.H. Greenland-Norway separation: A geodynamic model for the North Atlantic. Norwegian Journal of Geology 82, 281-298. Trondheim. ISSN 029-196X (2002).

Nauret F., Snow J. E., Hellebrand E., Weis D. Geochemical composition of K-rich Lavas from the Lena Trough (Arctic Ocean). Journal of Petrology 52, 1185–1206 (2011).

Neumann E. R., Schilling J. G. Petrology of Basalts from the Mohns-Knipovich Ridge – the Norwegian-Greenland Sea. Contrib. Mineral. Petrol. 85, 209–223 (1984).

Okino K., Curewitz D., Asada M., Tamaki K., Vogt P., Crane K. Preliminary analysis of the Knipovich Ridge segmentation: influence of focused magmatism and ridge obliquity on an ultraslow spreading system. Earth and Planetary Science Letters 202, 275-288 (2002).

Olesen O.G., Gellein J., Habrekke H. et al. Magnetic Anomaly Map, Norway and adjacent ocean areas, Scale 1:3 million. Geological Survey of Norway (1997).

Rudge, J. F., Maclennan, J., Stracke, A. The geochemical consequences of mixing melts from a heterogeneous mantle. Geochimica et Cosmochimica Acta, 114, 112-143 (2013).

Salters, V. J. M., Zindler, A. Extreme Hf-176 Hf-177 in the sub-oceanic mantle. Earth Planet Sci. Lett. 129, 13–30 (1995).

Salters, V.J.M., Dick, H.J.B. Mineralogy of the mid-ocean-ridge basalt source from neodymium isotopic composition of abyssal peridotites. Nature 418, 68–72 (2002).

Salters, V.J.M., Stracke, A., (2004). Composition of the depleted mantle. Geochemistry, Geophysics, Geosystems 5, Q05B07. doi:10.1029/2003GC000597.

Salters, V.J.M., Mallick, S., Hart, S.R., Langmuir, C.H., Stracke, A., 2011. Domains of depleted mantle; new evidence from hafnium and neodymium isotopes. Geochem. Geophys. Geosyst. doi:10.1029/2011GC003617 (2011).

Sanfilippo A., Salters VJM, Tribuzio R., Zanetti A. Role of ancient, ultra-depleted mantle in Mid-Ocean-Ridge magmatism. Earth and Planetary Science Letters, 511, 89–98 (2019).

Sani, C., Sanfilippo, A., Ferrando, C., Peyve, A., Skolotnev, S., Muccini, F., Zanetti, A., Basch, V., Palmiotto, C., Bonatti, E., Ligi, M. (2020) Ultra-depleted melt refertilization of mantle peridotites in a large intra-transform domain (Doldrums Fracture Zone; 7-8ºN, Mid Atlantic Ridge). Lithos (Impact factor: 3.39), 374-375: 105698, doi: 10.1016/j.lithos.2020.105698.

Sclater J. G., Anderson R. N., Bell H., Lee M. Elevation of Ridges and Evolution of the Central Eastern Pacific. Journal Geophysical Research 76, 7889-7915 (1971).

Schilling J. G., Zajac M., Evans R., Johnston T., White W., Devine J. D., Kingsley R. Petrologic and geochemical variations along the Mid-Atlantic Ridge from 29-degrees-N to 73-degrees-N. Am. J. Sci. 283, 510–586 (1983).

Schilling J. G., Kingsley R., Fontignie D., Poreda R., Xue S. Dispersion of the Jan Mayen and Iceland mantle plumes in the Arctic: a He–Pb–Nd–Sr isotope tracer study of basalts from the Kolbeinsey, Mohns, and Knipovich Ridges. J. Geophys. Res.-Solid Earth 104, 10543–10569 (1999).

Sokolov S.Y. Tectonic Evolution of the Knipovich Ridge Based on the Anomalous Magnetic Field. Doklady Earth Sciences 437, 343–348 (2011).

Sokolov S. Yu., Abramova A.S., Zaraiskaya Yu.A., Mazarovich A.O., Dobrolubova K.O. Recent Tectonics in the Northern Part of the Knipovich Ridge, Atlantic Ocean. Geotectonics, 48, 175–187. DOI: 10.1134/S0016852114030066 (2014).

Snow, J. E., Feldmann, H., Handt, A.V.D et al. Petrologic and tectonic evolution of the LenaTrough andWestern Gakkel Ridge. In: Bude.us, G. & Lemke, P. (eds) Reports on Polar and Marine Research. Bremerhaven: Alfred Wegener Institute for Polar and Marine Research. 153-208 (2007).

Stracke, A., Bourdon, B. The importance of melt extraction for tracing mantle heterogeneity. Geochim. Cosmochim. Acta 73, 218–238 (2009).

Stracke A., Snow J.E., Hellebrand E., von der Handt A., Bourdon B., Birbaum K., Gunther G. Abyssal peridotite Hf isotopes identify extreme mantle depletion. Earth Planet. Sci. Lett. 308, 359–368 (2011).

Stracke, A. Earth's heterogeneous mantle: a product of convection-driven interaction between crust and mantle. Chemical Geology, 330–331, 274–299 (2012)

Stracke A., Genske F., Berndt J., Koornneef J.M. Ubiquitous ultra-depleted domains in Earth's mantle. Nature Geosciences, 12, 851-855 (2019).

Sushchevskaya N.M., Peive, A. A., Belyatsky B.V. Formation conditions of slightly enriched tholeiites in the northern Knipovich Ridge. Geochemical Internaional 48, 321–337 (2010).

Trønnes R. G., Planke S., Sundvoll B., Imsland P. Recent volcanic rocks from Jan Mayen: low-degree melt fractions of enriched northeast Atlantic mantle. Journal of Geophysical Research-Solid Earth 104, 7153–7168 (1999).

Vogt P.R., Feden R.H., Eldholm O., Sundvor E. The Ocean Crust West and North of the Svalbard Archipelago: Synthesis and Review of New Results. Polarforschung 48, 1-19 (1978).

Waggoner D. An isotopic and Trace Element Study of Mantle Heterogeneity Beneath the Norwegian-Greenland Sea. University of Rhode Island, Kingston, RI, 270 (1989).

Warren, J. M., and S. B. Shirey. Lead and osmium isotopic constraints on the oceanic mantle from single abyssal peridotite sulfides. Earth and Planetary Science Letters 359, 279-293 (2012)

Warren, Jessica M. "Global variations in abyssal peridotite compositions." Lithos 248 (2016): 193-219

Willig M., Stracke A., Beier C., Salters V.J.M. Earth's chondritic light rare earth element composition: Evidence from the Ce–Nd isotope systematics of chondrites and oceanic basalts. Geochimica et Cosmochimica Acta, 272, 36-53 (2020).

Yampol’skiy K. P., Sokolov S. Y. Sedimentary Cover and Bouguer Anomalies in the Northern Part of the Knipovich Ridge. Doklady Earth Sciences 442, 188-192 (2012).

Zindler, A., Hart, S. Chemical geodynamics. Annual Review of Earth Planetary Science 14, 493–571 (1986).

Figure Captions

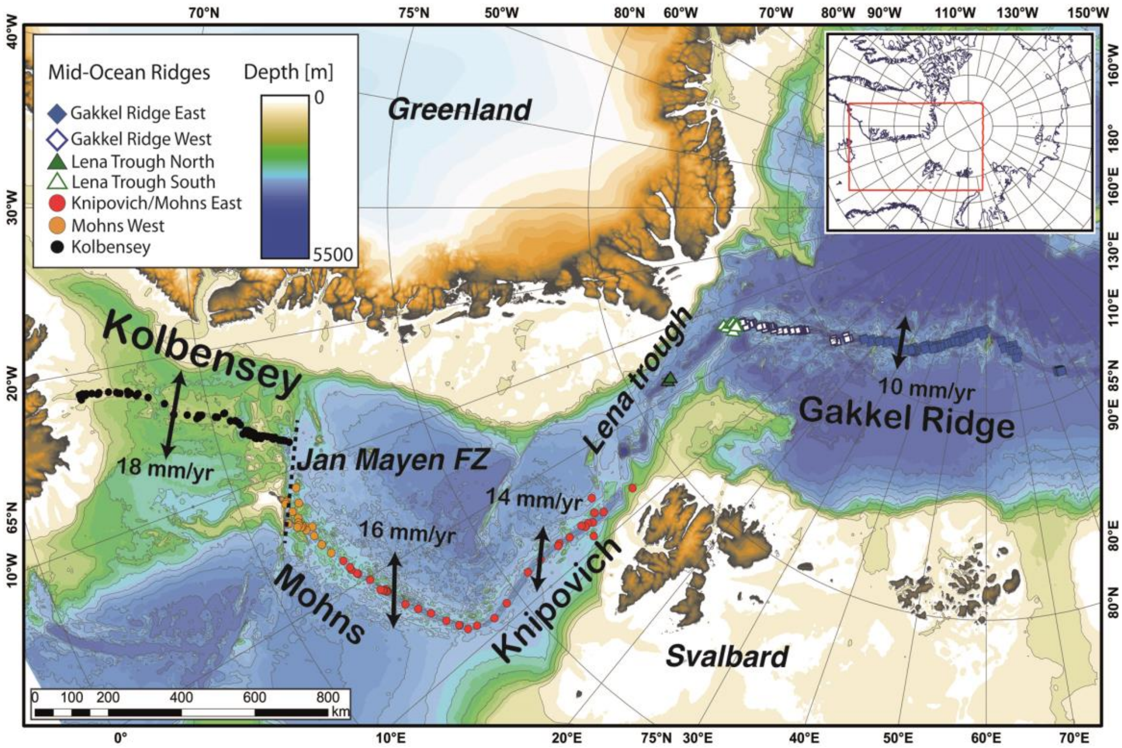

Figure 1. Orthostereographic projection of the Arctic region with the location of the basalts considered in this study along the Kolbensey, Mohns, Knipovich and Gakkel ridges and Lena Trough. Spreading rates and directions are from De Mets et al. (1990).

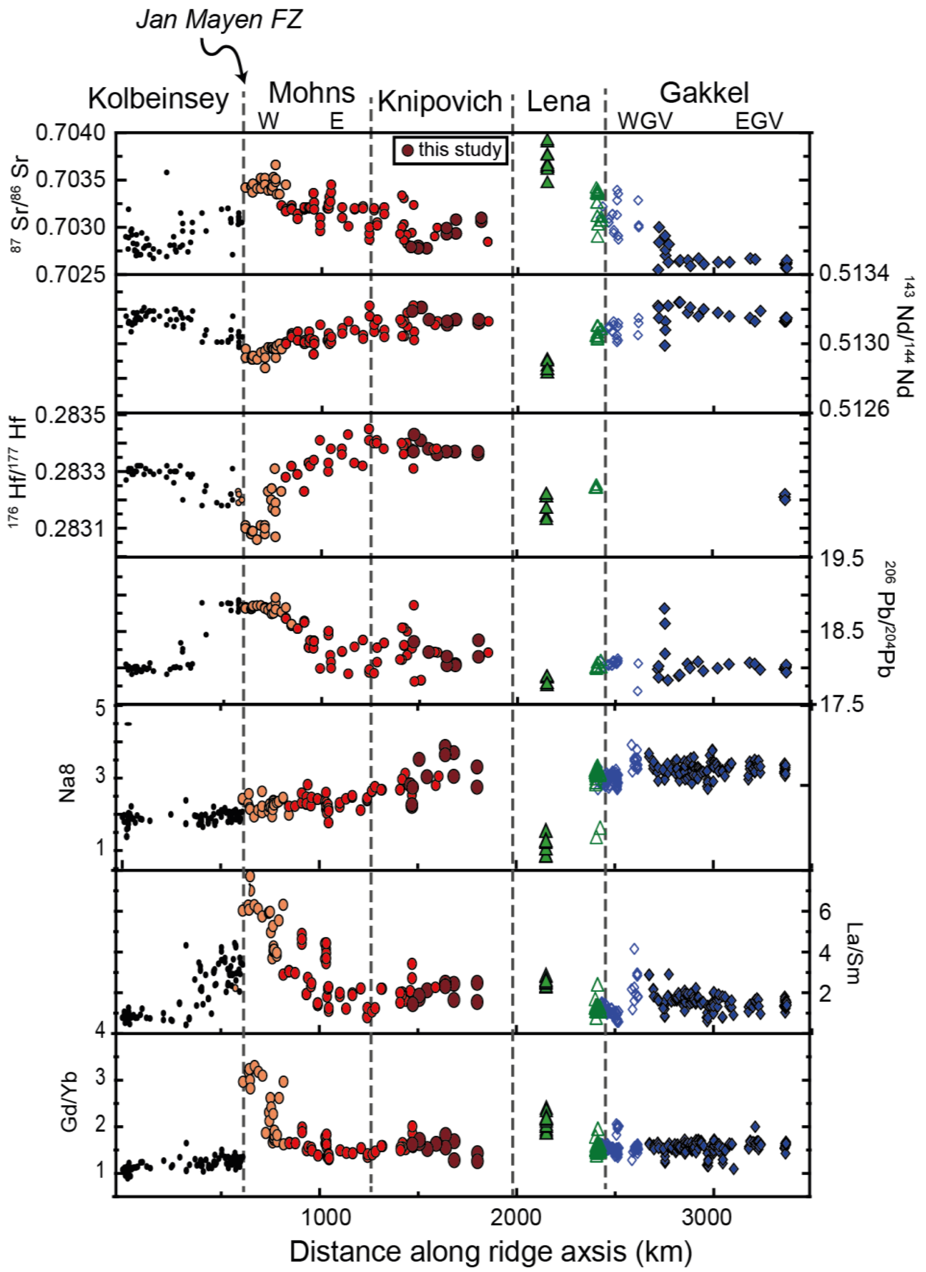

Figure 2. Along-axis geochemical composition of the basalts from the Arctic MAR. a) b) Sr-Nd-Hf-Pb isotope and La/Sm, Gd/Yb and Na8 compositions of basalts considered in this study as plotted along the cumulative distance along the spreading axis. Point 0 is located in the southernmost part of Kolbensey ridge. Also indicated the ridge names divided by fracture zones and the probable location of the Jan Mayen "plume-like" material. WGV and EGV indicate Western Gakkel and Eastern Gakkel volcanic zone, respectively (see Goldstain et al., 2008). Data reference in the text. Nd-Hf-Sr-Pb isotopes of basalts from the 77-79ºN region of Knipovich are from this study and reported in table S1.

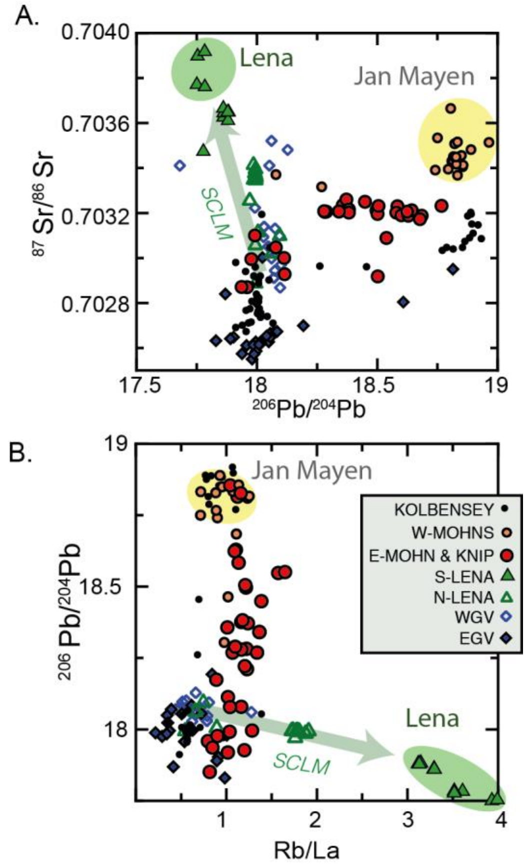

Figure 3. Possible contribution of a subcontinental lithospheric mantle in the basalts of the Arctic MAR. a) Sr vs Pb isotopes and b) Rb/La vs Pb isotopes. Green and yellow ovals include the enriched compositions of Lena Trough and Jan Mayen basalts. Also indicated the "dupal-type" anomaly depicted by Lena and WGV and defined by increasing Rb/La and Sr isotope at decreasing Pb (see Goldsteinet al., 2008). Although highly scattered, the basalts from Mohns and Knipovich follow a trend of enrichment pointing towards the enriched compositions of Jan Mayen (low Rb/La, high Sr and Pb isotopes), and diverging from enrichments typically related to a subcontinental lithospheric mantle (SCLM) component.

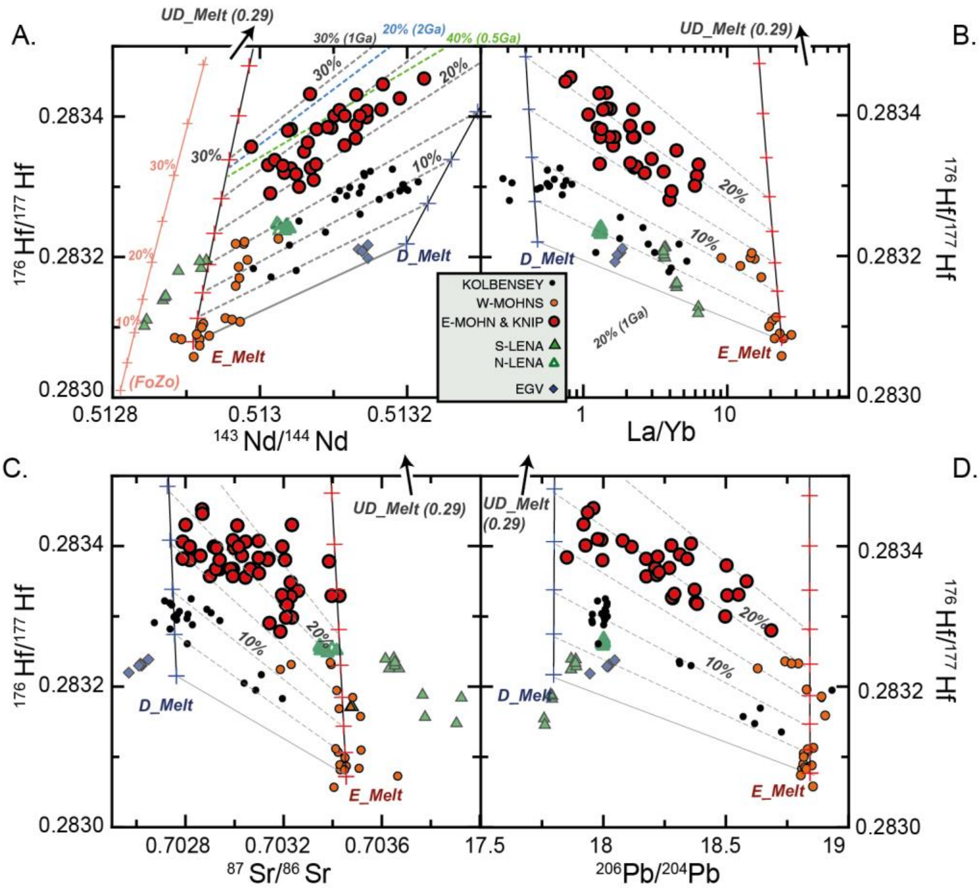

Figure 4. Co-variations in radiogenic isotope and incompatible trace elements of basalts from the Arctic MAR. Hf vs Nd (a), La/Yb ratio (b), Sr (c) and Pb isotopes (d). Symbols as in figure 1. The compositions of melts produced by our melting and mixing model are also plotted for comparison (see appendix for the model details and table S2 for melt compositions). The ultra-depleted melt (UD_melt) has Nd, Hf, Sr, Pb, thus plotting out of the plots. D_melt refers to MORB-like melt produced by 10% melting of a DM-like mantle source (DM composition from Salters and Stracke, 2004); E_melt EMORB-type melts similar to the average basalts from Jan Mayen island. Mixing lines produced by these three melt compositions are indicated by the steep lines in blue and red. Dashed lines depict the variability of melts produced at same proportion of UDmelt, representing lines with constant UD_Melt/(D_Melt + E_Melt) ratios (from 0 to 30%). These lines are parallel to the correlation lines seen in global MORB from different section of the Arctic MAR. The effect of a different time of depletion of the ultra-depleted mantle (0.5 Ga, 1 Ga and 2 Ga) and a E-melt with a more enriched compositions are also indicated in A. Whereas the effect of a more enriched source is negligible on the UD_Melt/(D_Melt + E_Melt) ratios, this has a strong dependence on the time of depletion of the ultra-depleted source (see text for further discussion).

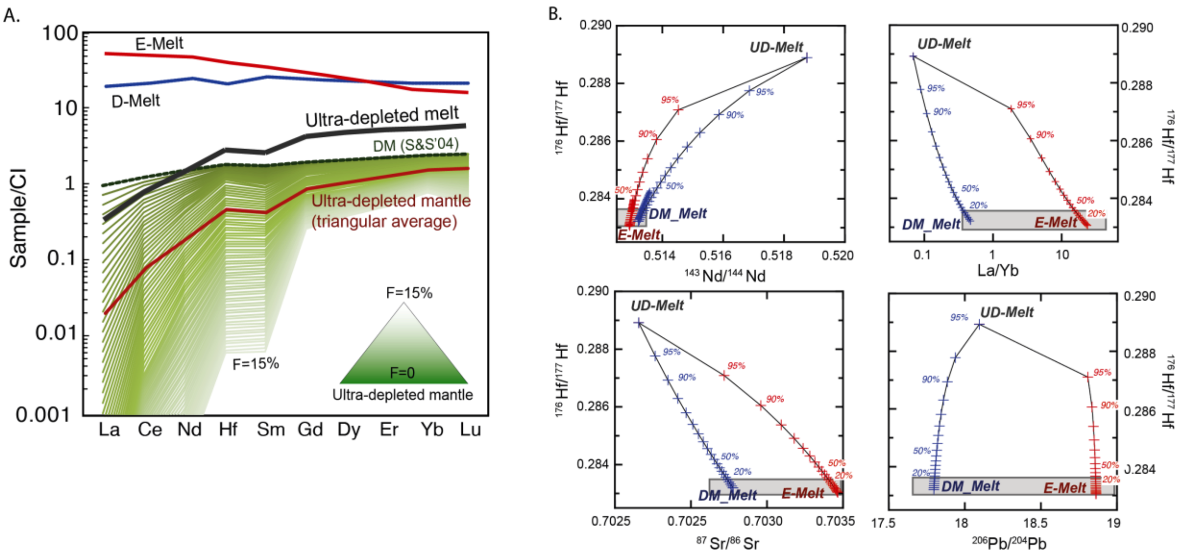

Figure 5. (a) Trace elements compositions of the mantle source and ultra-depleted melts resultant from the melting model. The average composition of the ultra-depleted mantle is calculated as weighted sum of intervals of F=0.2 and considering a triangular melting region (up to F=15%). (b) Large-scale view of the mixing trajectories between the three end-members melts in the Hf vs Nd-Sr-Pb isotopic spaces. The grey insets correspond to the areas in Figure 4.

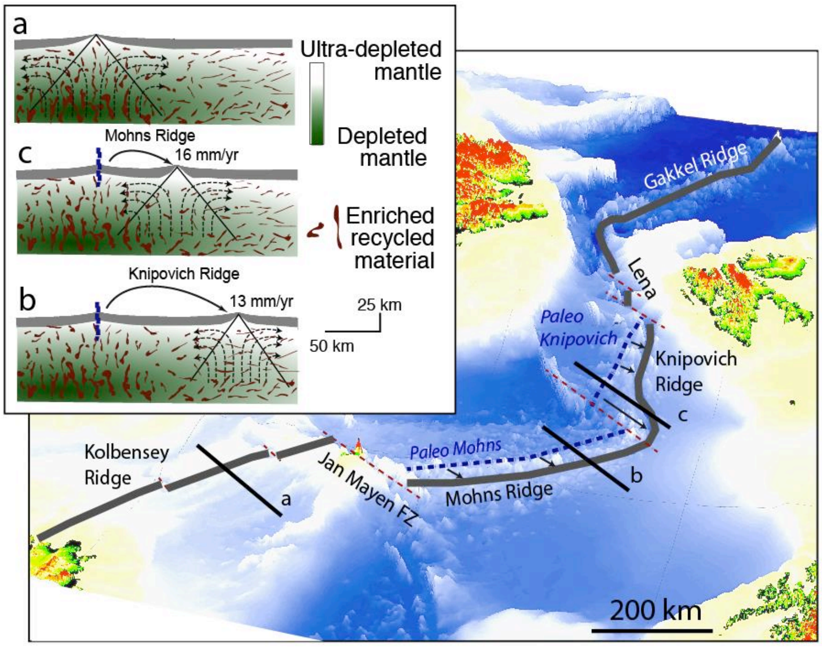

Figure 6. Three-dimensional visualization of the Arctic oceans and schematic representation of the ridge jump in Knipovich and Mohns ridges. The inferred positions of Paleo Knipovich and Paleo Mohns before ridge jump are indicated as blu lines (after Mosar et al., 2002; Sokolov et al., 2011). Solid black lines indicate the three profiles through the Kolbensey (a), Mohns (b) and Knipovich (c) ridges depicted in the inset. The inset shows three sections representing an idealized view of the asthenospheric mantle (redrawn after Liu et al., 2008; Sanfilippo et al., 2019; Sracke et al., 2019). Variably radiogenic mantle pockets (ranging from depleted to enriched in trace element and isotope compositions) are randomly distributed in a matrix formed by a depleted mantle possibly extending towards highly refractory compositions (ultra-depleted mantle, see text). During a first melting event, defined by a triangular melting region of a ~100 km depth, the amount of enriched material decreases, whereas the relative proportion of UDM/DM (depicted by the white-green color bar in the inset) increases. This refractory mantle will be emplaced at shallower depths, and transported laterally with the newly formed lithosphere (scheme a). If a rift jump occurs, this lithospheric mantle region is melted for the second time. Here, the proportion of UDM is higher, and its contribution becomes more noticeable in the erupted basalts. The ultra-slow spreading rates (indicated in figure) and the recent age of the ridge jumps (< 5 Ma) in Mohns and Knipovich allow this depleted portion of the mantle to melt substantially before new upwelling asthenosphere is emplaced in the melting region.

Figure 1

Click here to access/download;Figure;Fig.1.jpg

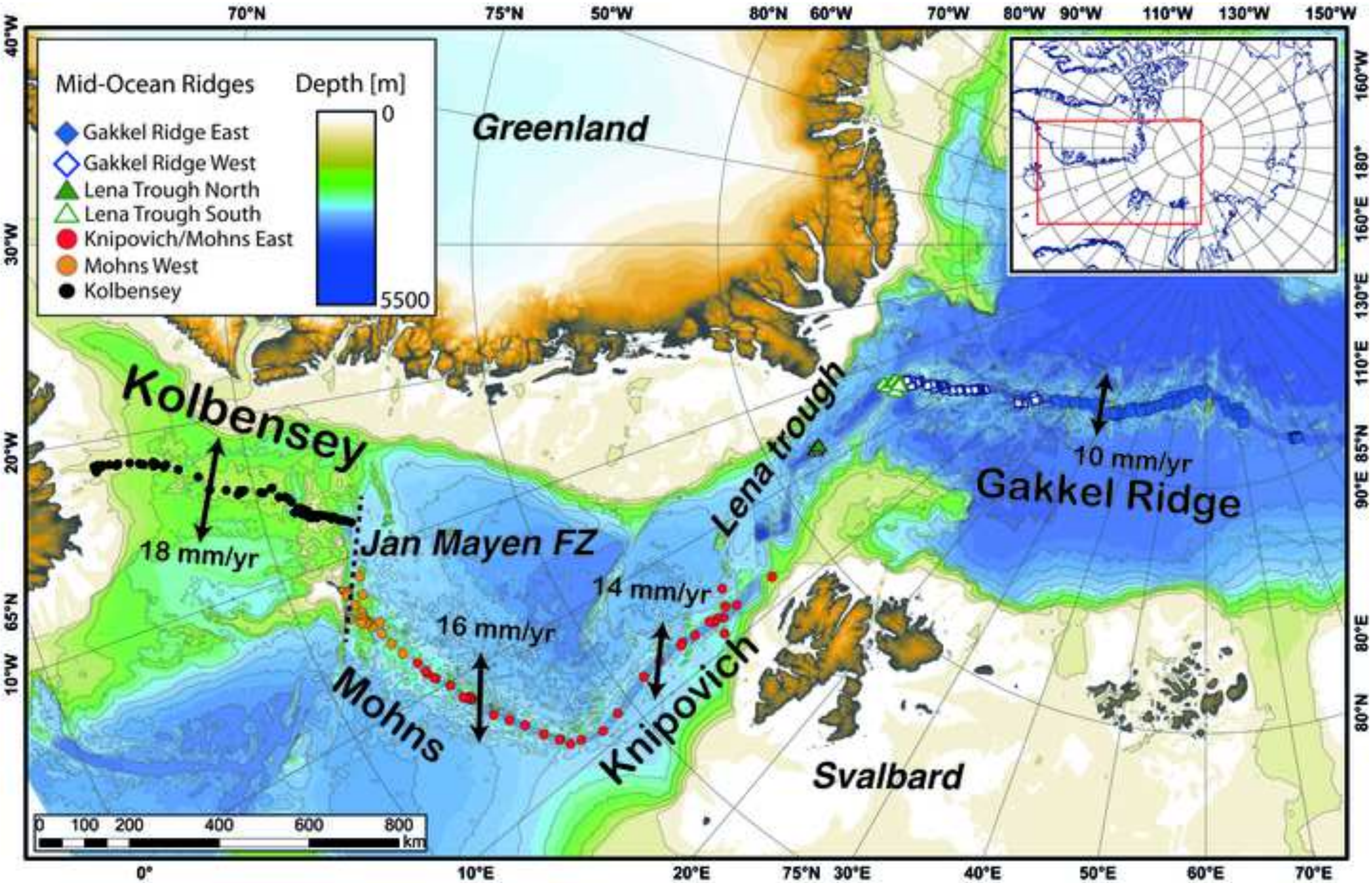

Figure 2

Click here to access/download;Figure;Fig.2.png

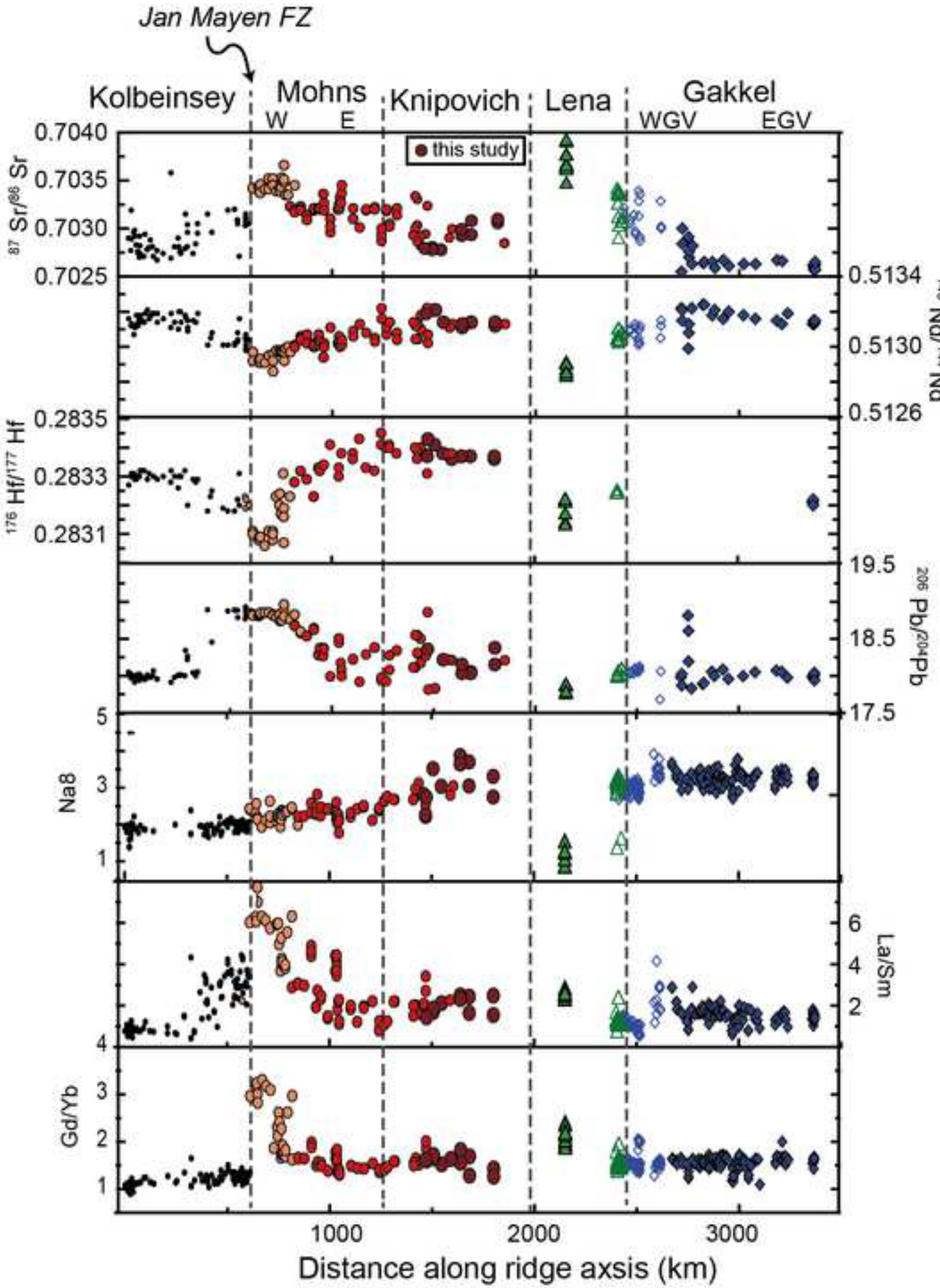

Figure 3

Click here to access/download;Figure;Fig.3.png

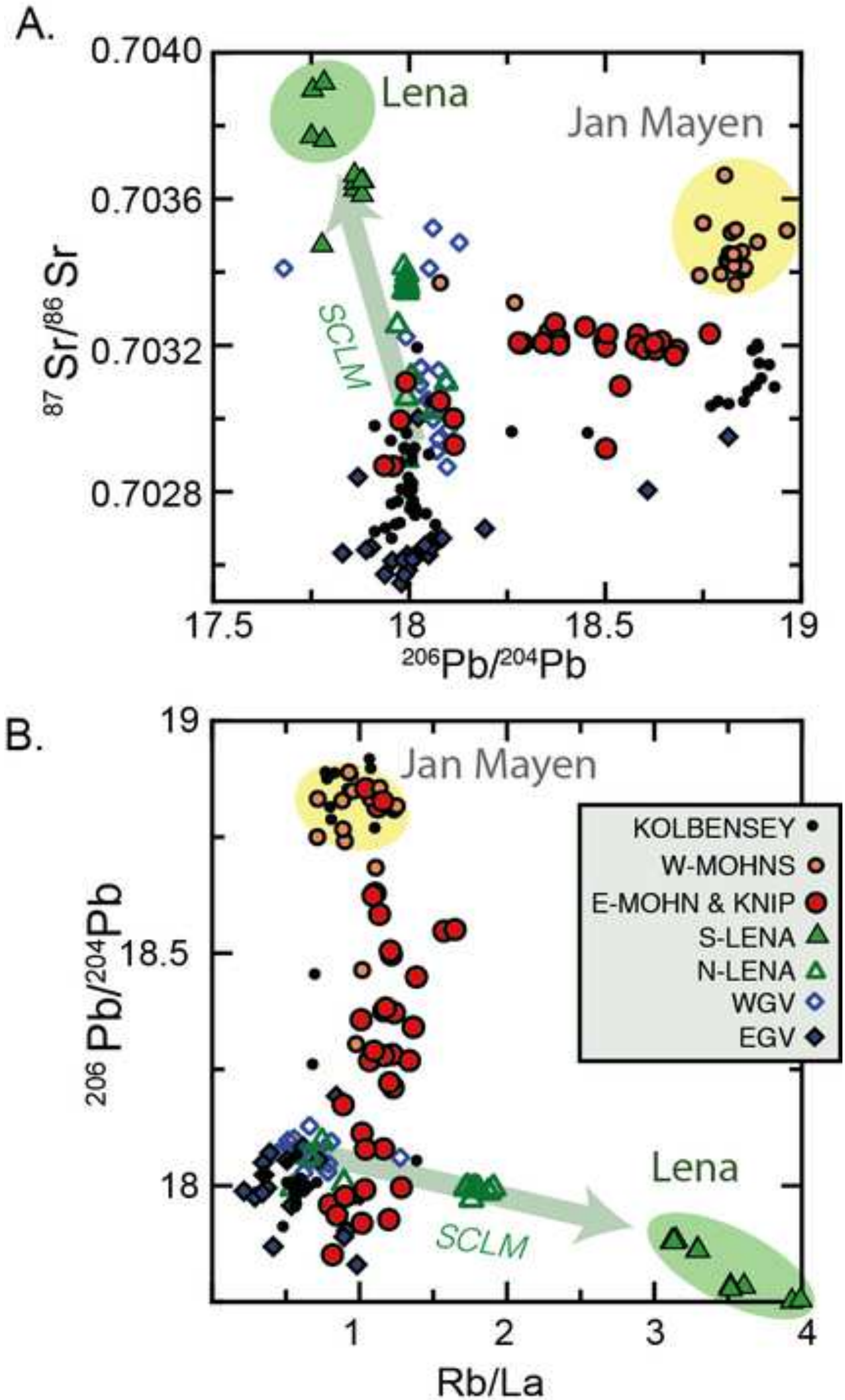

Figure 4

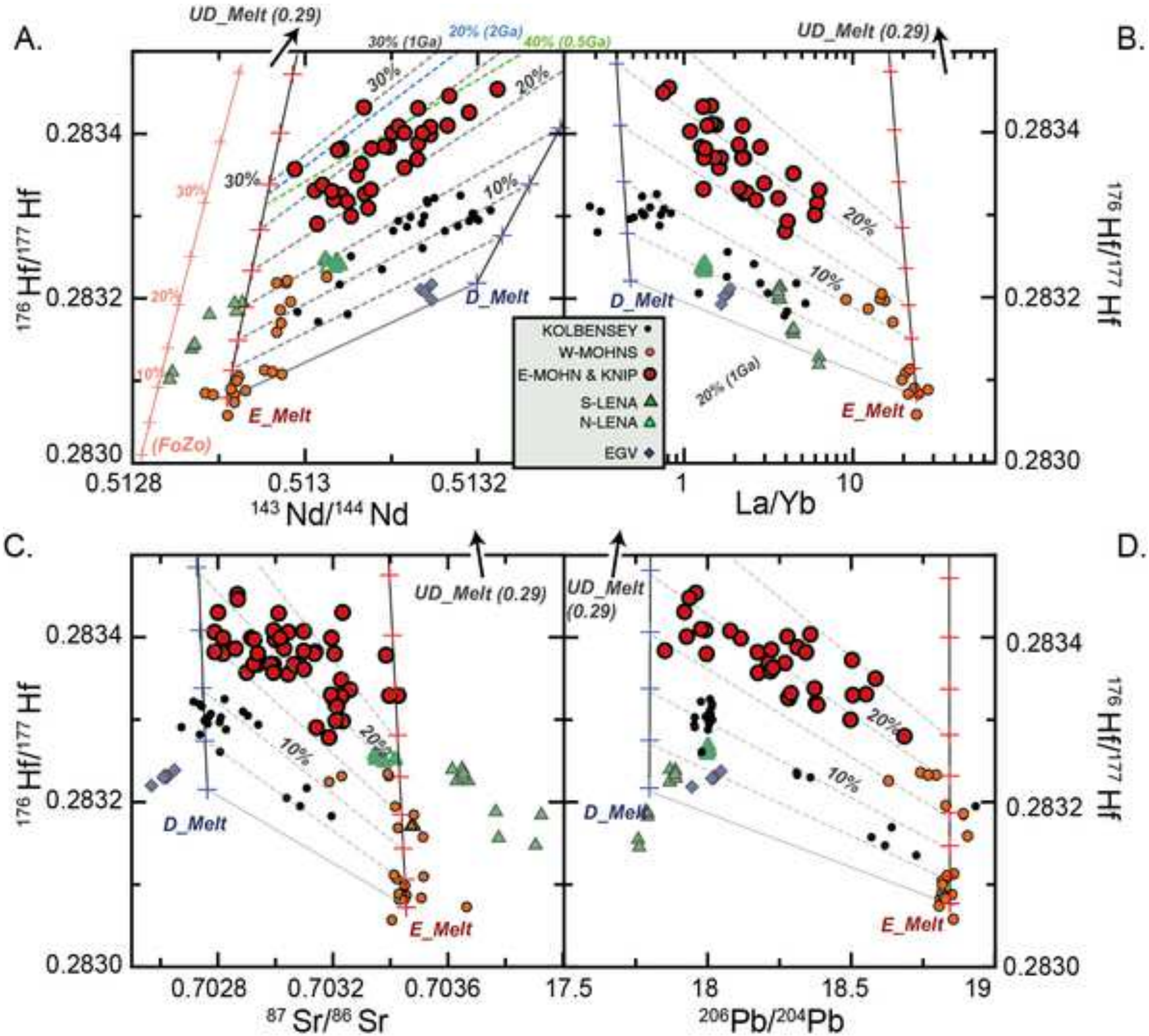

A.
B.
C.
D.
UD_Melt (0.29)
30% (1Ga)
20% (2Ga)
40% (0.5Ga)
30%
20%
10%
D_Melt
E_Melt
(FoZo)
20% (1Ga)
KOLBENSEY
W-MOHNS
E-MOHN & KNIP
S-LENA
N-LENA
EGV
176 Hf/177 Hf
143 Nd/144 Nd
La/Yb
87 Sr/86 Sr
206Pb/204Pb
0.2830
0.2832
0.2834
0.5128
0.513
0.5132
1
10
0.7028
0.7032
0.7036
17.5
18
18.5
19

Figure 5

Click here to access/download;Figure;Fig.5.png

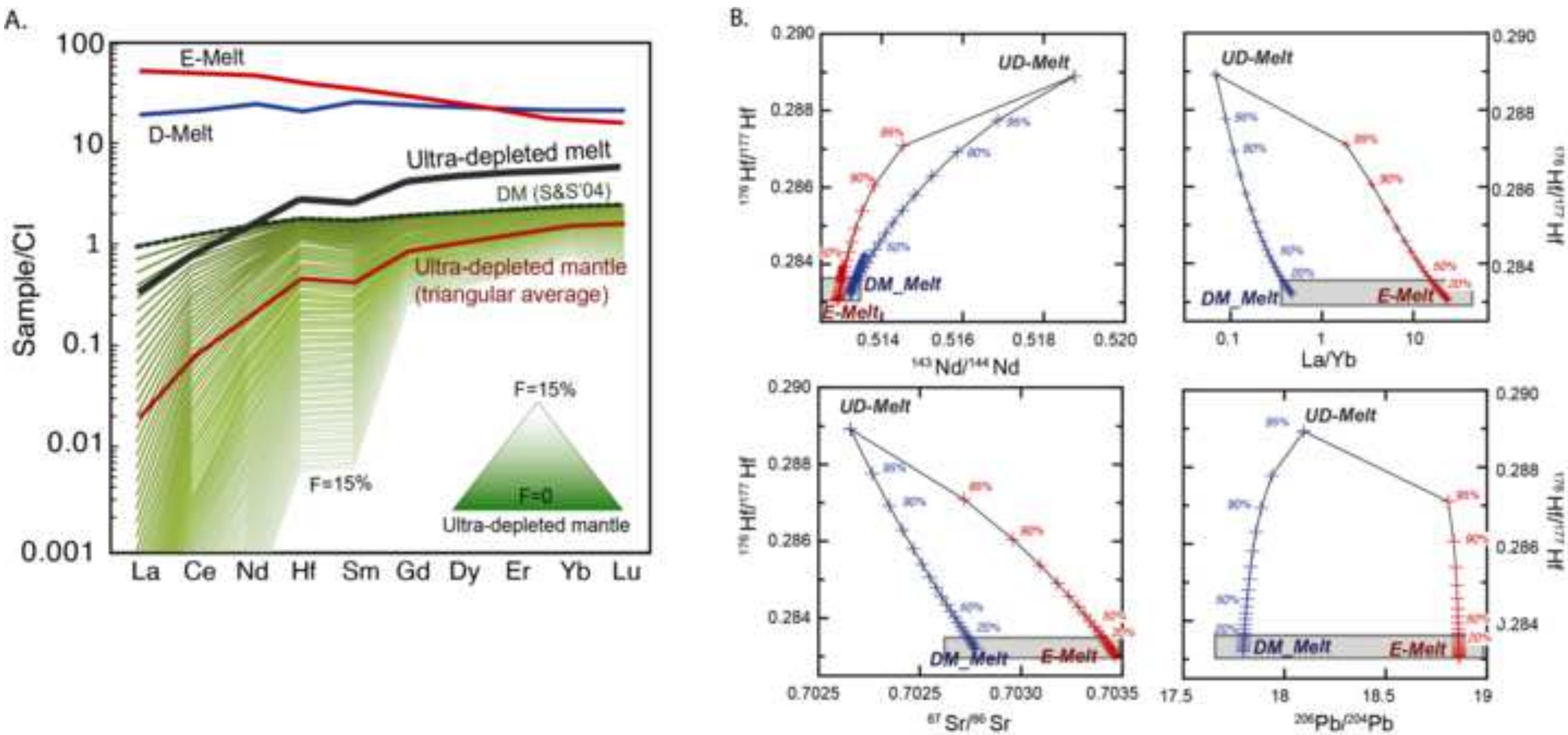

Figure 6

Click here to access/download;Figure;Fig.6.png

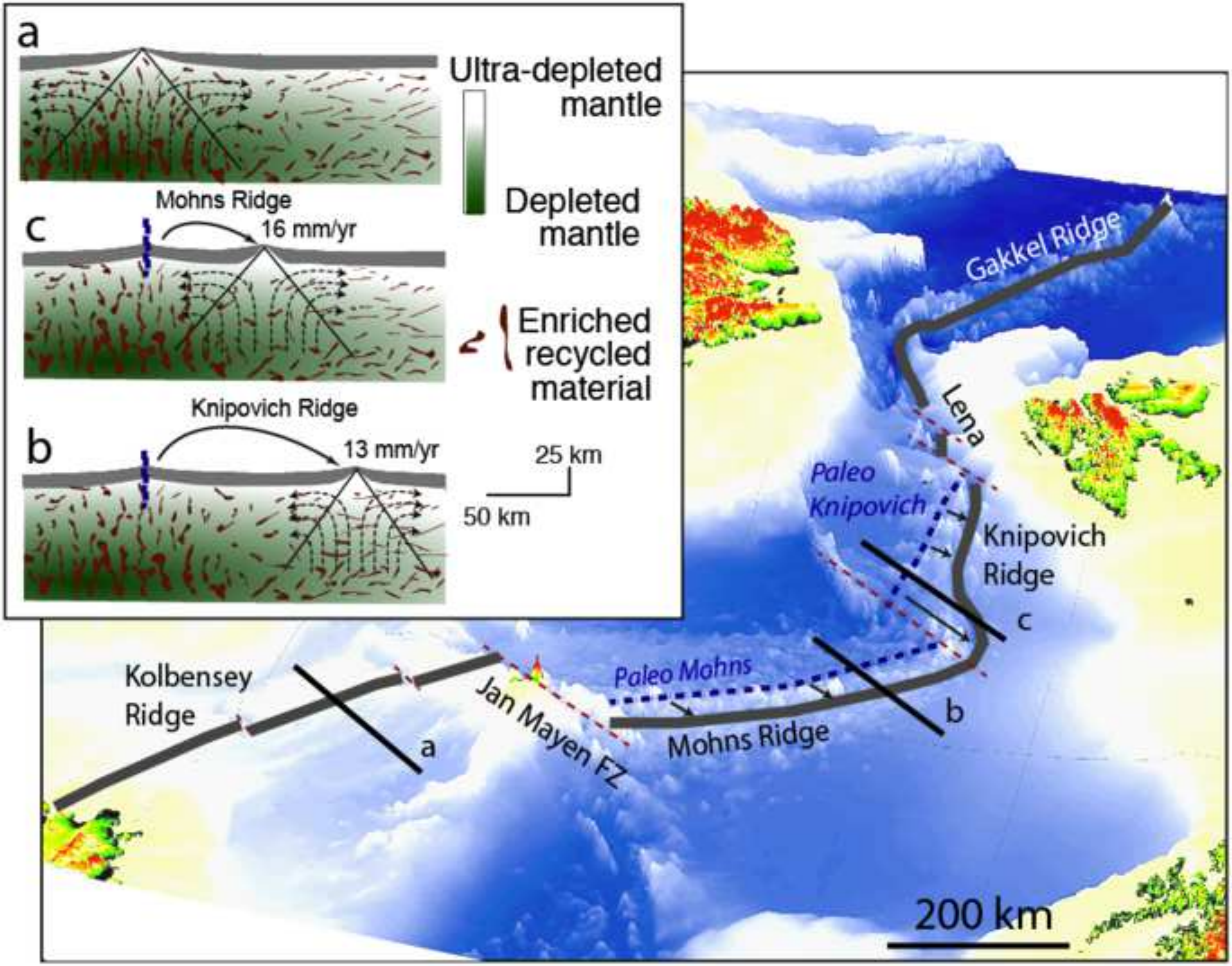

Table

Click here to access/download
Supplementary material for online publication only
Tables.xlsx

Supplementary material

Click here to access/download
Supplementary material for online publication only
Supplementary Material.docx

Author contributions: A.S, V.S and A.S. conceived the idea, performed the geochemical models and wrote the text; S.S. developed the geodynamic model; A.P. performed the preliminary petrological and geochemical study of the basalts; V.S. performed the isotopic determinations at FSU.

Declaration of interests

☒ The authors declare that they have no known competing financial interests or personal relationships that could have appeared to influence the work reported in this paper.

☐The authors declare the following financial interests/personal relationships which may be considered as potential competing interests: